Removal of methylene blue by orange and uvaia seeds

Bianca Mesquita Coelho Botrel[1], Zuy Maria Magriotis[1], Adelir Aparecida Saczk[1]*, Sabrina Mesquita Coelho[1], Priscila Ferreira de Sales[1]

[1]Federal University of Lavras (UFLA), Lavras – MG, Brazil.

Departament of Chemistry, Federal University of Lavras (UFLA), Lavras – MG, Brazil

biamesquitacoellho@yahoo.com.br, zuy@dqi.ufla.br, adelir@dqi.ufla.br,
sabrina10mcoelho@yahoo.com.br, priscila.ferreirasa@yahoo.com.br

ABSTRACT

In this study, the adsorption behavior of methylene blue (MB) was investigated using orange seed (OS) and uvaia seed (US) as low cost adsorbents. These materials were characterized using FTIR (Fourier transform infrared spectroscopy), elemental chemical analysis (CHNO), thermogravimetric analysis (TGA), zeta potential, specific surface area and a test for determination of acid sites. The parameters evaluated in the kinetic study of adsorption were contact time, initial dye concentration, mass of adsorbent and pH. The adsorption of MB onto OS and US samples could be explained by Elovich´s kinetic model. The experimental isotherms data, carried out at the temperatures of 25°C, 35°C, 45°C and 55°C, were better represented by Sips. It was verified that the adsorption was spontaneous and endothermic according to the thermodynamic parameters $\Delta G°$, $\Delta H°$ and $\Delta S°$ evaluated. The OS and US maximum adsorption capacity at the temperature of 25°C was 38 mg g^{-1} and 48 mg g^{-1}, respectively. The reuse tests performed at three subsequent times showed that there was no significant decrease regarding the materials efficiency, therefore emphasizing its viability as biosorbents.

Indexing terms/Keywords

Adsorption. Agroindustrial wastes. Methylene blue. Orange seed. Uvaia seed.

Academic Discipline And Sub-Disciplines

Chemistry, Physical Chemistry

1 INTRODUCTION

As the population has been growing continuously, most common environmental issues from industrial processes, agriculture, mining, and domestic activities have been observed [1]. For instance, the textile dyeing industry consumes large quantities of water and produces large volumes of wastewater from different steps. These substances are very rich in colors and it is generally applied at food, cosmetics, leather, and pharmaceuticals among other industries segments [2].

Despite the high applicability, most dyes contain chemicals that can harm human health and the environment and the biological stability of the molecules makes it hard to be degraded by conventional treatment systems used by industries [3].

Due to the intense coloration, the passage of solar radiation may be restrict, decreasing natural photosynthetic activities and letting to changes in the aquatic biota [4]. Dye methylene blue belongs to the thiazines class and it is widely used as a model molecule for pollution indicator as well as studies of mesoporosity and functional groups [5].

The chemical, biological, and electrochemically assisted photocatalytic degradation of reactive dyes [6, 7], the precipitation processes and photo-Fenton [8,9] are examples of varieties of several decontamination methods for the removal of pollutants from effluents. However, adsorption is one of the most studied methods since it produces a high quality treated effluent. It also has low cost, it is ease to operate and there are possibilities of reusing the water and the adsorbent that can be recycled afterwards [10].

Activated carbon is the most used adsorbent by the industry. However, it has some disadvantages related to production costs and low regenerability [11]. Therefore, researches have been conducted regarding the development of alternative adsorbent materials. For example, agroindustrial wastes such as corncobs [12], cane bagasse [13], coconut fibers [14], coffee beans [15] have been studied with the aim of employing efficient, low cost regenerable adsorbents.

Orange cultivation plays a very important economic role, being one of the most cultivated and consumed fruit in the world. The Brazilian citriculture stands out as one of the main economic activities, driving the country's economy expressively. The uvaia is another fruit which presents high industrial potentialities, once they are used in the manufacture of juices, liquors, jellies, and others. However, most part of these fruits, including shells, bagasse and seeds, are not reused in the process. In this way, this work aims at studying the efficiency of orange seed (OS) and uvaia seed (US) as adsorbent materials in the adsorption of MB dye, potentially adding value to these wastes.

2. MATERIAL AND METHODS

2.1 Preparation of adsorbents

The samples of OS and US were dried for 16 h at 40° C, ground and sieved to pass through a 0.425 mm sieve (35 Tyler series).

2.2 Characterization of adsorbents

An Elementar Analysensysteme vario MICRO cubeTM was employed to determine the percentages of C, H, N, S and O (by difference) in OS and US. Thermogravimetric analyses were performed using a Shimadzu model DTG-60AH thermomechanic analyzer (Shimadzu model DTG-60AH) and were carried out under a nitrogen atmosphere in the temperature range of 25–900 °C at a heating rate of 10 °C min^{-1}. Fourier transform infrared spectroscopy (FTIR) in the 400 to 4000 cm^{-1} range a Bruker Vertex 70V. Microscopic observations and electron micrographs were made using a Nano Technology Systems model Evo® 40 VP SEM. For the purpose of determining zeta potentials, adsorbents were ground (< 37 μm particle size), the suspensions adjusted to the required pH (in the range of 2–11) and sedimented/conditioned for 2 h at 22 ^{o}C in 250 mL erlenmeyer flasks containing sodium nitrate solution (0.002 mol L^{-1}) as supporting electrolyte. Potentials were measured using a Zeta Meter System 3.0+ ZM3-D-G instrument. The applied tension varied between 75 and 200 mV, and zeta potentials were expressed as the average values of 20 repetitions. Acidity was determined using 0.1 g of the adsorbents and 20 mL of potassium hydroxide solution (0.01 mol L^{-1}). The system was maintained at a resolution of 4 cm^{-1}, using KBr pellets (300 mg of KBr to 3 mg of was carried out sample). The analyses were carried out using at 25 ^{o}C on an orbital shaker (50 rpm) for 3 hours, followed by titration with hydrochloric acid solution (0.01mol L^{-1}).

2.3 Preparation of dye solutions

The adsorption tests were carried out using the methylene blue dye (MB) (VETEC) as adsorbate. The different concentrations tested in the experiments were diluted from a 2 g L^{-1} stock solution of MB. The natural pH values of the stock solution was 5.5, and it was adjusted (when necessary) by adding either potassium hydroxide 0.01 mol L^{-1} or hydrochloric acid 0.01 mol L^{-1}. The structural formula of MB, properties and characteristics are described in Table 1.

Table 1 Properties and characteristics of MB

Generic name	Methylene blue
Chemical name (IUPAC)	3.7-bis(dimethylamino)-phenothiazin-5-ium chloride
CASnumber	61-73-4
C.I.*	52015
Chemical formula	$C_{16}H_{18}ClN_3S$
Molecular weight (g mol^{-1})	319.85
Chemical structure	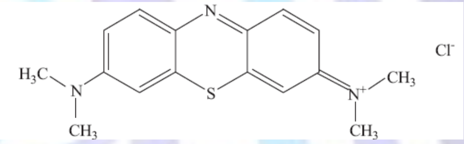

2.4 Adsorption experiments

A monitored 24-hour analysis was carried out to determining the equilibrium time. For this, 10 mL of methylene blue solution at an initial concentration of 25 mg L^{-1} at natural pH was placed on contact with 0.1 g of each adsorbent (US and OS).

To establish the influence of the initial concentration, solutions at concentrations corresponding to 25, 50 and 100 mg L^{-1} were used at an adsorbent mass/adsorbate volume ratio of 1:100 (0.1 g of adsorbent).

In order to study the adsorbent mass/adsorbate volume ratio, 10 mL of methylene blue solution, at natural pH were placed in contact with 0.2, 0.1 and 0.05g of adsorbent, which led to ratios of 1:50, 1:100 and 1:200, respectively.

The last parameter analyzed was the influence of pH. For that, a solution of methylene blue was prepared at an optimized initial methylene blue concentration, adjusting the pH to 3, 4, 7, 8 and 9, using acetic acid or potassium hydroxide solution 0.1 mol L^{-1}.

The resulting mixtures were maintained at room temperature (25±1 ^{o}C) on an orbital shaker (200 rpm). The supernatants were then separated by centrifugation (5 min at 1540 x g) and diluted (when necessary) so that the remaining concentrations of MB could be determined at 665 nm, using a Femto model 800 XI UV-vis spectrometer.

The dye removal percentage (%) was calculated by using the following equation 1:

$$\%R = \frac{C_o - C_t}{C_o} x100 \qquad (1)$$

where C_o is the initial dye concentration (mg L^{-1}) and C_t is the dye concentration (mg L $^{-1}$) at time any time. All the samples were analyzed in duplicate to ensure data reproducibility.

2.5 Adsorption isotherms

The adsorption isotherms were constructed using optimized parameters. For this, solutions of adsorbate (MB) at concentrations ranging from 10 to 2000 mg L^{-1} were prepared. The quantity of dye adsorbed by mass of OS and US at equilibrium was determined from the equation:

$$Q_e = \frac{(C_o - C_e)V}{m} \qquad (2)$$

where Q_e (mg g^{-1}) is the quantity of MB adsorbed by the mass of OS and US at equilibrium, C_o is the initial and C_e is the concentration at equilibrium of MB (mg L^{-1}), V is the volume of the solution (L) and m is the mass of adsorbent (g). All experiments were carried out in duplicate.

2.6 Thermodynamics of the adsorption process

The temperature effect on the adsorption of MB on OS and US was studied at temperatures of 25 ^{o}C, 35 ^{o}C, 45 ^{o}C and 55 °C. The thermodynamic parameters enthalpy (ΔH°), entropy (ΔS°) and Gibbs free energy (ΔG) can be calculated from equations 3, 4 and 5.

$$\Delta G^\circ = -RT \ln K_L \qquad (3)$$

$$\Delta G^\circ = \Delta H^o - T\Delta S^o \qquad (4)$$

$$\ln K_L = \frac{\Delta S^\circ}{R} - \frac{\Delta H^\circ}{RT} \qquad (5)$$

where K_L represents the Langmuir equilibrium constant (L mol^{-1}), R the universal gas constant (8.314 J mol^{-1} K^{-1}) and T the temperature in Kelvin (K). The values of ΔH^o and ΔS^o were obtained from the curve fitting coefficients of the graphic ln K_L versus 1 / T.

2.7 Reuse test

The desorption of the amount of MB adsorbed on OS and US samples was carried out using HCl 0.1 mol L^{-1} solution and an adsorbent mass (g), in a ratio of 1:10. The systems were kept under agitation for 2 hours at 120 rpm and at the end of each experiment the supernatants were collected and the amount of dye removed was then determined by UV-Vis spectroscopy at 665 nm. The adsorbents were water-washed, vacuum filtered and placed in an oven at 50 °C for 2 h for drying. The regenerated adsorbents were used in three subsequent adsorption-desorption cycles.

3. RESULTS AND DISCUSSION

3.1 Characteristics of the absorbents

The direct (TGA) and differential (DTG) thermogravimetric curves for OS and US show that mass loss occurred at three different stages in both adsorbents, with similar characteristics (Figure 1). The initial loss of mass at approximately 100 ^{o}C was associated with the elimination of water and small volatile molecules, while the second reduction occurred between 300 and 350 ^{o}C and was caused by the thermal degradation of cellulose and hemicelluloses. The final mass loss at approximately 400 ^{o}C may be attributed to the degradation of lignin, which has a much higher thermal stability than either cellulose or hemicellulose polymers. The greatest rate of mass loss occurred at the latter temperature [16].

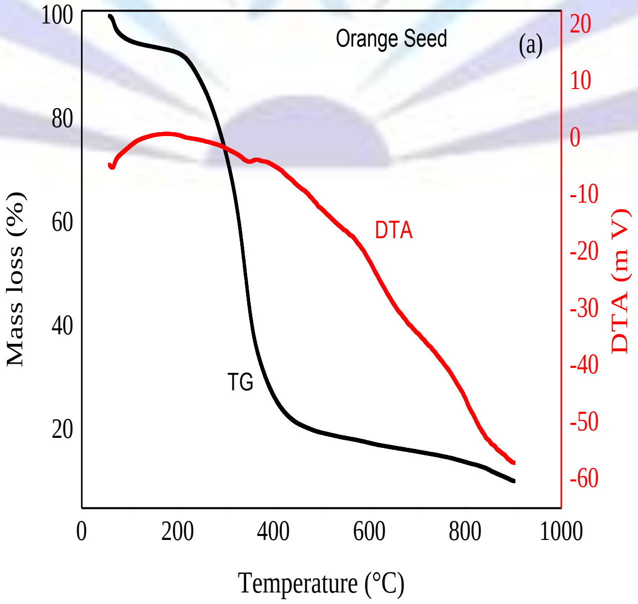

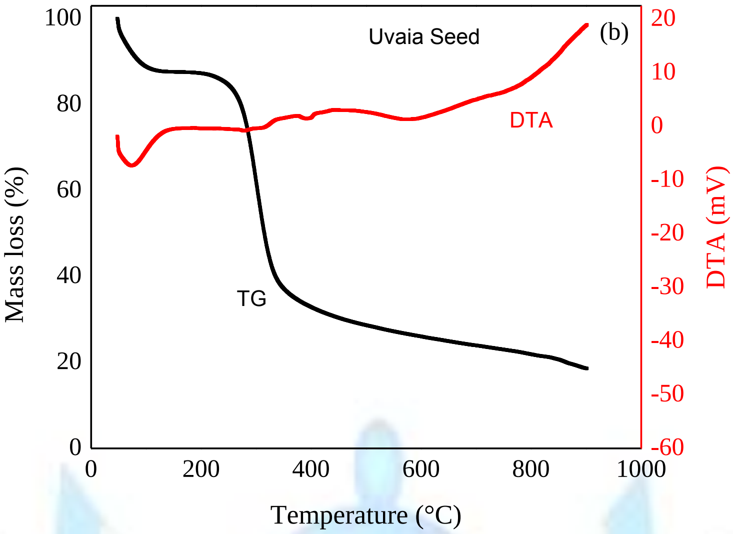

Figure 1. Direct (TG: -) and differential (DTA-) thermogravimetric curves for OS (A) and US (B).

The elemental composition (Table 2) indicates that the adsorbents materials were rich in oxygen but contained low levels of sulfur. Both seeds presented similar C/ H ratio. However, for C/O, US had a significantly smaller ratio compared to OS.

Table 2 Elementar chemical composition of the samples OS and US

Adsorbent	C (%)	*O (%)	H (%)	N (%)	S (%)	Relation C/H	Relation C/O
OS	47.38	43.72	6.43	2.40	0.073	7.4	1.1
US	38.89	53.28	5.75	2.04	0.045	6.8	0.73

*The percentage of O was obtained by difference

The FTIR spectrum of OS and US (Figure 2) showed a broad peak at 3400 cm^{-1} indicating hydroxyl groups, characteristic of OH stretches corresponding to pectin, cellulose, water, hemicellulose and lignin [17,18]. The bands located at 2931 cm^{-1} and 2924 cm^{-1} can be assigned to the CH stretching of methyl and methoxy groups. The band identified at about 1744 cm^{-1} confirms the presence of the carbonyl group (C = O) that extends to vibrations of carboxyl groups present in hemicellulose, pectin and lignin. The band located at 1638 cm^{-1} was attributed to the stretching of C = C bound constituents of the aromatic benzene molecules or rings in lignin. The bands located between 1300 and 1000 cm^{-1} can be attributed to the stretching of CO bound corresponding to vibrations of carboxylic acids and alcohols. The bands near to 600 cm^{-1} confirm the presence of ethers sand lactones

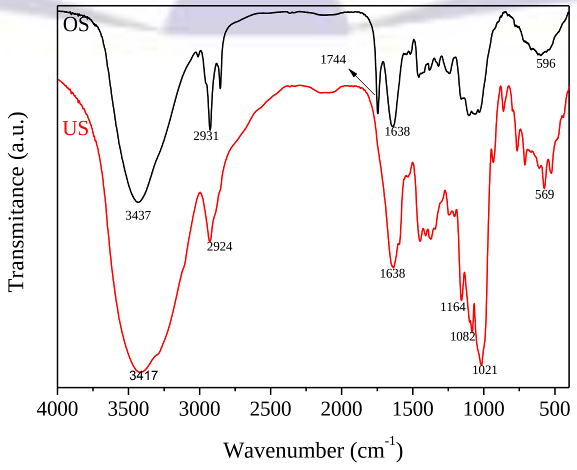

1].

Figure 2. FTIR spectra of OS and US

The adsorbent materials were submitted to chemical titration of acid ligand sites. The results indicated that OS had an acidity corresponding to 3.11 mmol g $^{-1}$, which was higher than the US (up to 2.78 mmol g^{-1}). The high acidity found in the materials can be attributed to the presence of Bronsted acidic groups (carboxylic acid and alcohols) identified in the FTIR analysis.

Zeta potential is a measurement of the superficial charge of the adsorbent at a specific pH and indicates which type of ion would be adsorbed under such conditions. As shown in Figure 3, both OS and US presented negative surface charges throughout the pH range studied (3.0–10.5), meaning that both adsorbents would exhibit a great affinity for cations. The negative charge present on the surface of lignocellulosic materials is associated with acidic entities such as carboxyl and phenolic OH groups.

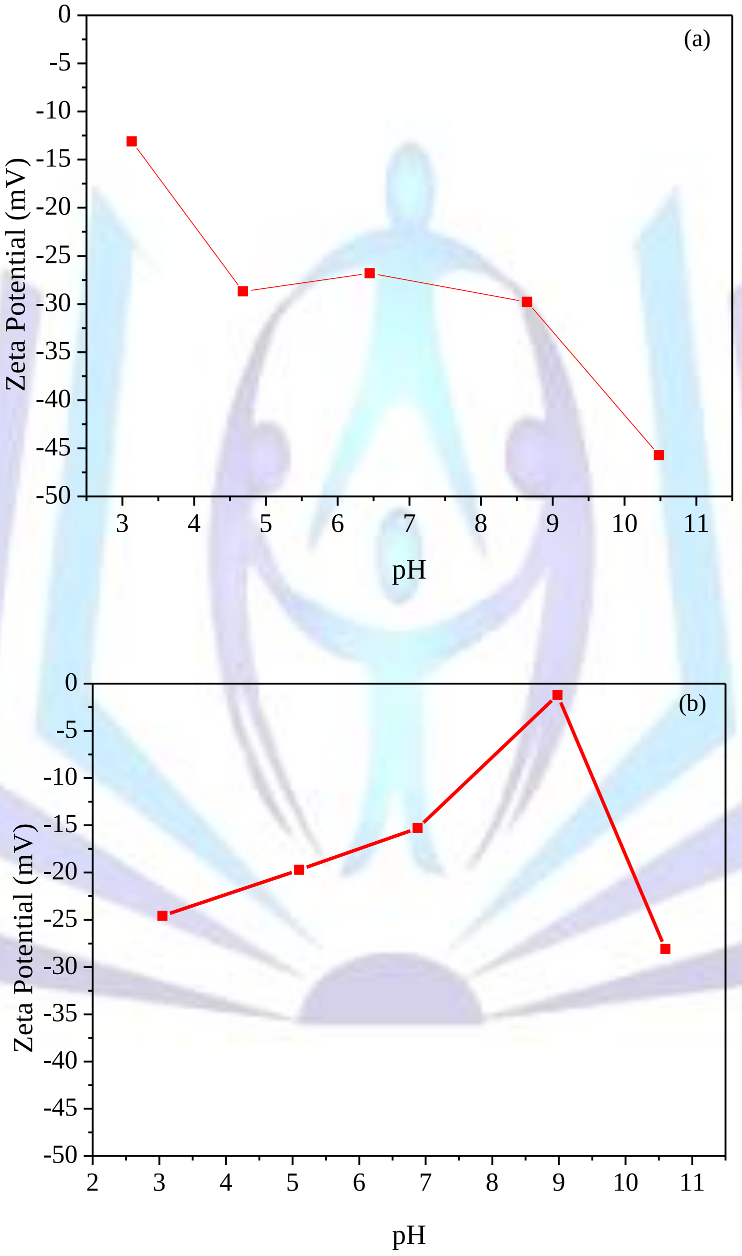

Figure 3. Zeta Potential of OS (A) and US (B)

3.2 Influence of physicochemical parameters on adsorption

The rates of adsorption of MB as a function of time of contact with the absorbent are shown in Figure 4. As observed, the equilibrium times for OS and US were 4 and 8 hours, respectively. The difference in the equilibrium times of the adsorbent materials can be attributed to the bio-sorbents chemical composition as well as the adsorption sites accessibility.

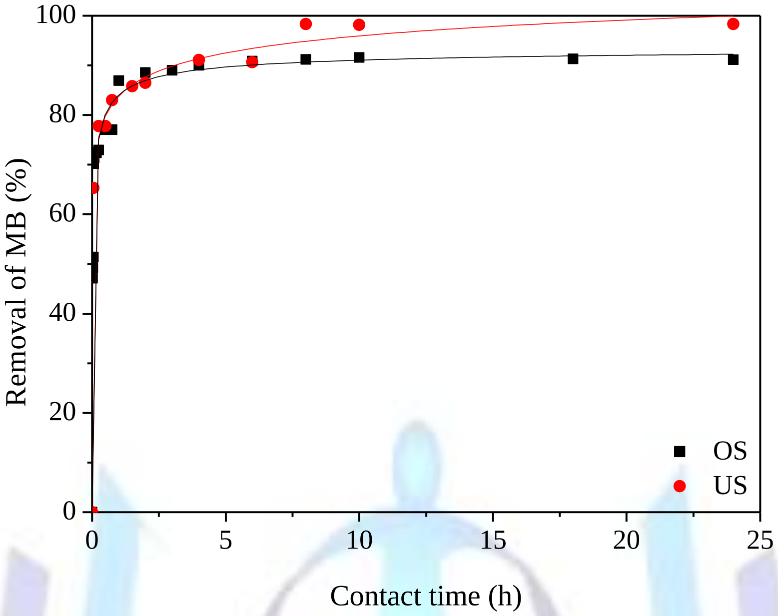

Figure 4. Influence of the contact time on the adsorption of MB by OS and US

The analysis results show that an increase of the initial concentration of the dye reduced the adsorption the adsorbents capacities, but this parameter was most significant for US sample. The lowest removal when higher concentrations were used can be attributed to difficulties in diffusion capacity of the adsorbate molecules or even the competition among the molecules that are being adsorbed on the active surface sites of the adsorbent material [19].

The study of the mass of bio-sorbents (Figure 5) showed that the optimal amounts for continuing the adsorption process were 0.1 g and 0.05 g for OS and US, respectively.

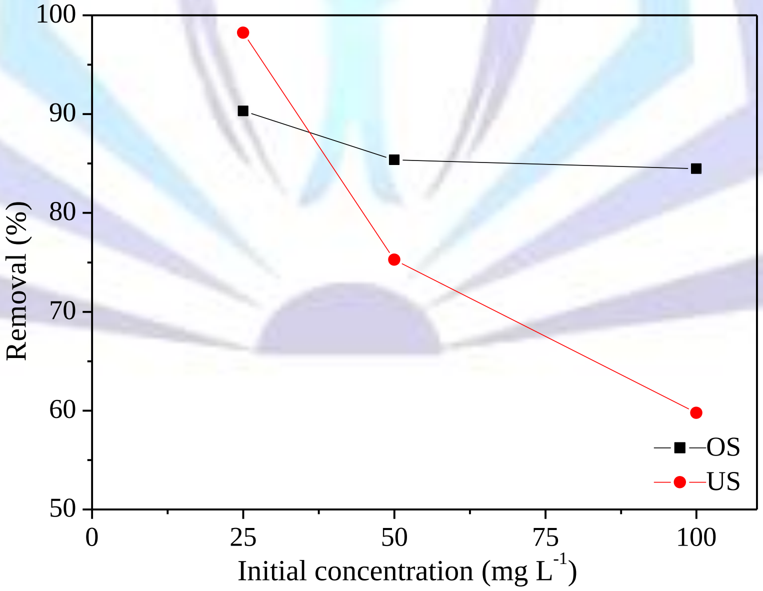

Figure 5. Influence of the initial concentration on the adsorption of MB

The influences of variable pH values are shown in Figure 6. It is observed that for both bio-sorbents a lower percentage removal of dye occurred at low pH values (pH 3 and 4), which can be attributed to the association of H3O+ ions with the adsorbents surface, limiting the approximation of MB, which is cationic dye [20]. There was an increase in adsorption capacity at pH 5.5 (natural) and above this there is a significantly decrease in the adsorption process efficiency.

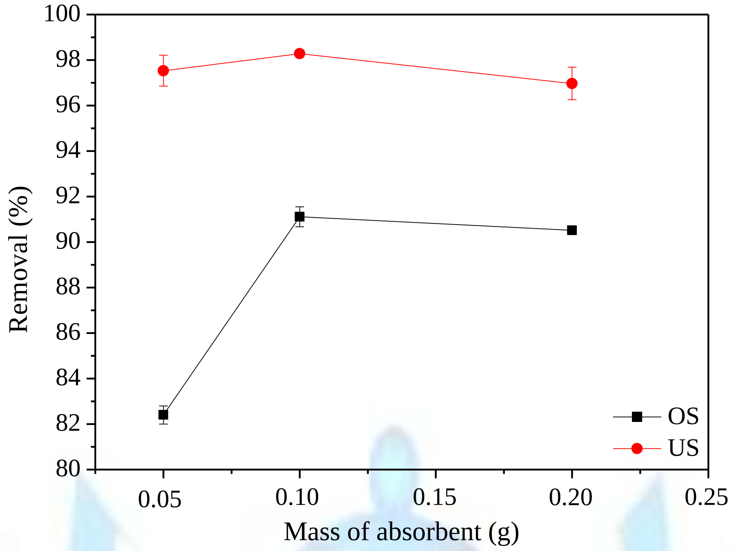

Figure 6. Influence of the weight of adsorbent on the adsorption

Optimized conditions were considered for the subsequent analysis. For this, aliquots of MB 25 mg L^{-1} and pH 5.5 were placed in contact with 0.1 and 0.05g of both adsorbents OS and US.

3.3 Kinetic characteristics of the adsorbents

The kinetic parameters of adsorption of MB onto OS and US were determined under optimized conditions. The data were analyzed using models represented mathematically by non-linear equations of Table 3.

Table 3 Kinetics models non-linear

Models	**Equations**
Pseudo-first order [27]	$q_t = q_e(1-e^{k_1 t})$
Pseudo-second order [28]	$q_t = \dfrac{q_e{}^2 k_2 t}{1+Q_e k_2 t}$
Intra-particle diffusion [29]	$q_t = k_{ID}\sqrt{t} + C$
Elovich [30]	$q_t = \dfrac{1}{\beta}\ln(t+t_0) - \dfrac{1}{\beta}\ln(t_0)$
Avrami [31]	$q_t = q_e\left\{\ 1-\exp\left[-(k_{AV}t)\right]^{n_{AV}}\right\}$

Where, q_t is the amount of dye removed in time t (mg g^{-1}), q_e is the amount of dye removed at equilibrium (mg g^{-1}), k_1 is the rate constant of pseudo first order (h^{-1}), t is the contact time, k_2 is the constant of pseudo second order (g $mg^{-1}h^{-1}$), k_{ID} is the rate constant of intra-particle diffusion, C is the constant related to the diffusion layer thickness, β is the relation between the surface coverage degree and the activation energy involved in the chemisorption, t_0 is the initial time , k_{AV} is the Avrami kinetic constant and n_{AV} is a constant related to the kinetics of adsorption reactions.

It was observed that the experimental data of the adsorbents OS and US were better fitted to the kinetic model described by Elovich (Figure 7 and Table 4). The proposed model describes the adsorption maintained by chemisorption in heterogeneous surfaces in a process relatively slow and justified by the equilibrium times of 4 and 8 hours to OS and US samples, respectively [21].

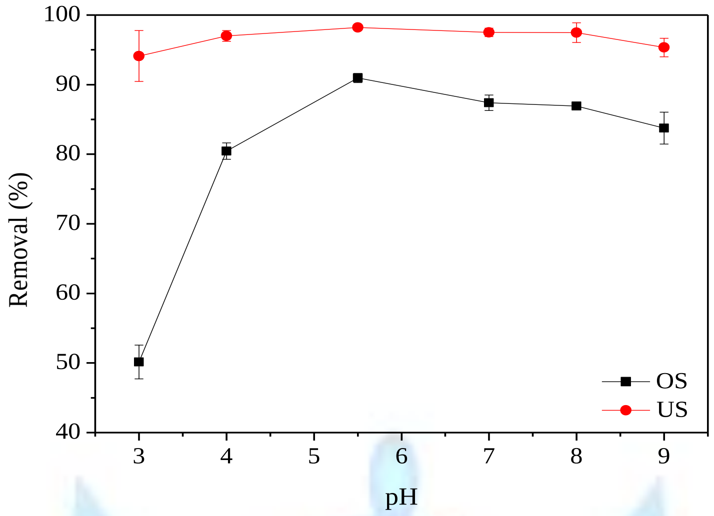

Figure 7. Influence of pH on the adsorption

Table 4 Adjustment of the experimental data to the kinetic models non-linear

Kinetic Model	OS	US
Pseudo-first Order	r^2=0.8984 q_e=2.0308 k_1=29.0429 Error=0.2006	r^2=0.9037 q_e=4.4600 k_1=10.8316 Error=0.4497
Pseudo-second Order	r^2=0.9492 q_e=2.1293 k_2=22.9273 Error=0.1418	r^2=0.9621 q_e=4.7369 k_2=3.6631 Error=0.2802
Intraparticle diffusion	r^2=0.5306 C=1.2000 k_{ID}=0.6976 Error=0.4312	r^2=0.4953 C=2.5777 K_{ID}=0.2019 Error=1.0523
Elovich	r^2=0.9574 β=5.0879 Error=0.1299	r^2=0.9803 β=2.3165 Error=0.2075
Avrami	r^2=0.8984 q_e=2.0300 k_{AV}=3.9912 n=7.2767 Error=0.2095	r^2=0.9037 q_e=4.4600 k_{AV}=1.3664 n=7.9268 Error=0.4770

3.4 Adsorption isotherms of the adsorbents

The adsorption isotherms of OS and US for the removal of MB under optimized conditions are shown in Figure 8. The data obtained were fitted to the isotherm models represented, mathematically, using non-linear equations (Table 5).

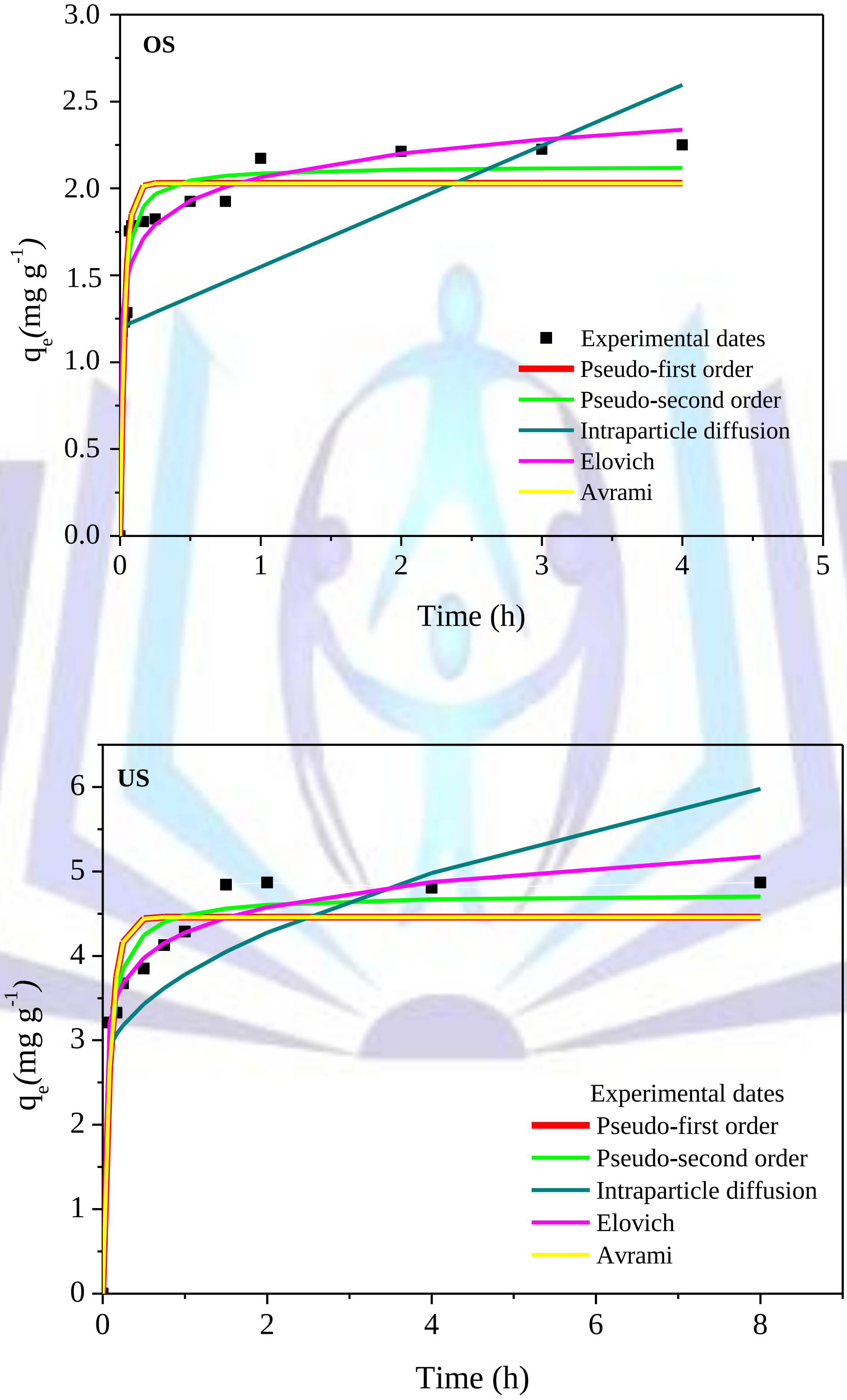

Figure 8. Fits of the kinetic models for OS and US

Table 5 Kinetics models non-linear equations

Models	Equations
Langmuir [32]	$q_e = \frac{q_m K_L C_e}{1 + K_L C_e}$
Freundlich [33]	$q_e = K_F C_e^{1/n}$
Sips [34]	$q_e = \frac{q_m K_s C_e^{1/m}}{1 + K_s C_e^{1/m}}$
Dubinin-Radushkevich [35]	$q_e = q_m \exp\left(-b_{DR}\left[RT\ln\left(1+\frac{1}{C_e}\right)\right]^2\right)$

Where, q_e is the amount of adsorbate adsorbed per unit of adsorbent mass at equilibrium (g g^{-1}), q_m is the adsorption capacity of the monolayer (L mg^{-1}), K_L is the equilibrium constant (L mg^{-1}), C_e is the adsorbate solution concentration at equilibrium (mg L^{-1}), K_F is the Freundlich constant ($mg^{1-1/n}$ kg^{-1} $L^{1/n}$) , 1/n represents the adsorption intensity, K_S is the Sips equilibrium constant related to the adsorption energy (L $mg^{-1})^{1/m}$, 1/m is the Sips model exponent that characterizes the system heterogeneity, b_{DR} is the constant of adsorption energy (mol^2 K J^{-2}), R is the gases universal constant (kJ mol^{-1} K^{-1}), T is the temperature (K).

The parameters results obtained to adsorption in OS and US are shown in Table 6.

Table 6 Isotherms and parameters for adsorption of MB onto OS and US

Adsorbent	**Isotherm**	**T(K)**			
		298	**308**	**318**	**328**
OS	**Langmuir**				
	q_m (mg g^{-1})	42.18	74.19	61.68	65.07
	K_L (L mg^{-1})	0.0127	0.0030	0.0317	0.0092
	r^2	0.9884	0.9959	0.9950	0.9961
	Standard error	2.4899	2.1675	2.6387	2.1961
	Freundlich				
	K_F (mg g^{-1}) (L $mg^{-1})^{1/n}$	4.3913	1.1492	10.0186	5.2559
	n	3.0424	1.7158	3.6606	2.8185
	r^2	0.9438	0.9811	0.9470	0.9719
	Standard error	5.2805	4.6189	8.4992	5.8672
	Sips				
	q_m(mg g^{-1})	40.5654	61.4299	63.1248	68.4758
	K_S	0.0085	0.0005	0.0396	0.0110
	n	0.8986	0.7084	1.0925	1.0594
	r^2	0.9891	0.9987	0.9954	0.9984
	Standard error	2.4608	1.3008	2.6749	1.4762

	Dubinin-Radushkevich				
	b ($mmol^2J^{-2}$)	0.0002	0.0023	0.000028	0.0005
	q_m($mg\ g^{-1}$)	34.24	50.05	52.90	54.01
	r^2	0.9662	0.9884	0.9592	0.9522
	Standard error	4.1172	3.6221	7.4821	7.6153
US	**Langmuir**				
	q_m ($mg\ g^{-1}$)	52.99	47.33	49.22	52.36
	K_L ($L\ mg^{-1}$)	0.0900	0.3944	0.0988	0.4183
	r^2	0.9890	0.9818	0.9905	0.9956
	Standard error	3.3025	4.3690	3.2214	2.2455
	Freundlich				
	K_F ($mg\ g^{-1}$)($L\ mg^{-1}$)$^{1/n}$	6.1889	14.7625	13.2705	18.1337
	n	3.5090	4.5725	5.0103	6.1000
	r^2	0.9340	0.9702	0.9542	0.9130
	Standard error	7.9699	5.5806	7.0292	9.7607
	Sips				
	q_m ($mg\ g^{-1}$)	48.8067	58.2246	51.4554	50.8908
	K_S	0.0005	0.3070	0.1627	0.3916
	n	0.6100	1.8793	1.3481	0.8622
	r^2	0.9946	0.9938	0.9927	0.9950
	Standard error	2.4517	2.8110	3.0370	0.8367
	Dubinin-Radushkevich				
	b ($mmol^2J^{-2}$)	0.0009	7.5109	3.0945×10^{-6}	3.5444×10^{-7}
	q_m($mg\ g^{-1}$)	46.88	51.38	46.69	48.79
	r^2	0.9851	0.9170	0.9781	0.9867
	Standard error	3.8333	9.1846	4.8883	3.8841

According to the correlation coefficients, it was verified that the data were better fitted to the Langmuir and Sips models to OS and US at all temperatures. Although the determination coefficients were close, the Langmuir model showed the highest standard error value. Thus, the experimental data have were better fitted to the Sips model (Figure 9). These results confirm the superficial heterogeneity of adsorbent materials when using the methylene blue dye as adsorbate [22, 23].

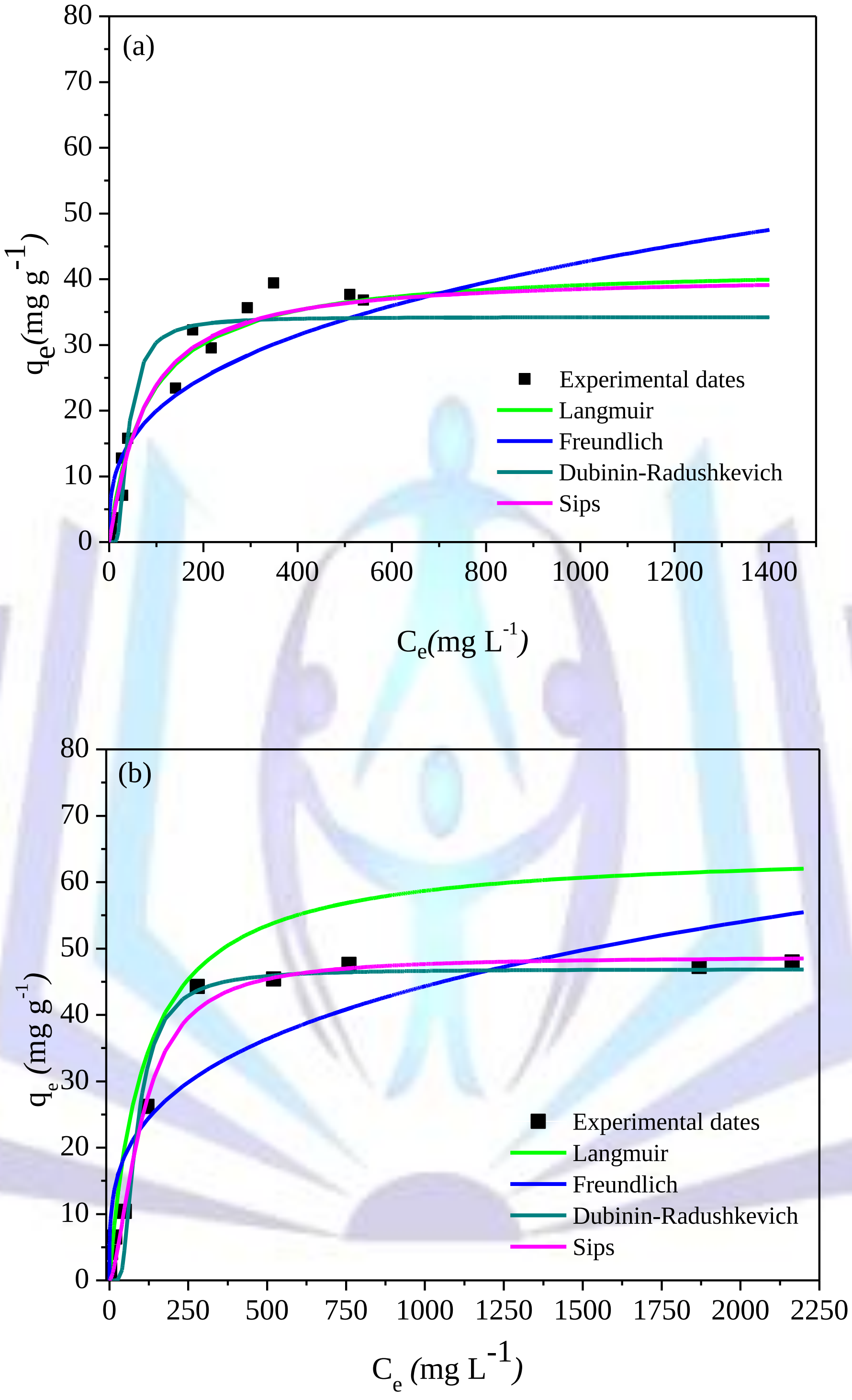

Figure 9. Fits of the isotherm models for OS (A) and US (B) at 25°C

The maximum adsorption capacity (q_m) of US with respect to MB was greater than that of OS (48.80 and 40.60 mg g^{-1}, respectively). These results are within the range found in the literature for other plant residues studied by other authors including Neem (Azadirachta indica) leaf poder (8.76 mg g^{-1}), Banana peel (15.9 mg g^{-1}), Orange peel (17.6 mg g^{-1}), Olive Stones (22.1 mg g^{-1}) Macauba palm cake (27.75 mg g^{-1}) and Paspalumnotatum (31.0 mg g^{-1}).

3.5 Thermodynamic studies

The results obtained to the MB adsorption onto OS and US conduced at different temperatures are shown in Table 7.

Table 7 Thermodynamic parameters calculated for the adsorption of MB by OS and US

T(K)	q_{mexp} (mg g^{-1})	$q_{m\ Lang}$ (mg g^{-1})	K_L (L mg^{-1})	ΔG° (kJ mol^{-1})	ΔH° (kJ mol^{-1})	ΔS° (J mol^{-1})
		OS				
298	37.97	42.18	0.0127	-19.54	11.15	102.99
308	52.67	74.19	0.0030	-20.57		
318	59.89	61.67	0.0317	-21.60		
328	61.39	65.07	0.0092	-22.63		
		US				
298	47.61	52.99	0.0090	-22.03	83.55	354.30
308	50.56	47.33	0.3944	-25.57		
318	48.96	49.22	0.0988	-29.12		
328	51.13	52.36	0.4183	-32.66		

As it can be seen, the values of $q_{m,exp}$ increased with the increasing temperature, which characterizes an endothermic process in OS and US, justified by the ΔH° positive values for both adsorbents. The ΔHo values between 40 and 120 kJ mol^{-1} reinforce the chemisorption characteristic. It was observed with increasing temperature that the Gibbs free energy became more negative, indicating an increase in the adsorption process spontaneity for both seeds. The ΔS° positive value to the dye adsorption in both seeds show an increase in entropy (or disorder) in the solid / liquid interface, as a result of MB adsorption [24]. Increasing adsorption with increasing temperature can be attributed to the adsorption sites dilation.

The increase in the adsorbate molecules diffusion in the external boundary layer and also inside the adsorbent inner layer are due to a decrease in the solution viscosity and an increase of the dye molecules mobility, which obtains an appropriate kinetic energy to interact with the OS and US surfaces. These results suggest that the processes involve chemisorption in adsorbents. Similar results have also been observed in other studies performed with different materials [25,26].

3.6 Specific surface area of the adsorbents

Values for the specific surface area of the adsorbent were calculated from the following equation [17]:

$$S = q_m N_A /(MM_{MB})\sigma_{MB} \qquad (6)$$

where q_m is the maximum adsorption capacity (mg g^{-1}), N_A is Avogadro's number (6.022 ×1023 mol^{-1}), MM_{MB} is the molecular weight of MB (319.85 g mol^{-1}) and σ is the area occupied by a single adsorbed MB molecule (130Å^2). Considering the experimental results and that the area occupied by an adsorbed molecule of this dye is 130 Å^2, the specific surface area of the adsorbents OS and US (estimated by Eq. 6) were 91.48 e 116.48 m^2 g^{-1}, respectively.

3.7 Adsorbent materials reusing test: desorption

The results of the three adsorption/desorption cycles showed that the removal efficiency of the dye was reduced by 24% (from 90% to 69%) and 10% (from 97% to 87%) to the OS and US, respectively. The results showed that the US had higher regenerative capacity, allowing it to be a good source suitable to being used as an adsorbent material.

4. Concluding Remarks

The uvaia seed (US) was more efficient than the orange seed (OS) in the removal of methylene blue. Both materials are very promising in the removal of contaminants from aqueous effluents. Further, after three consecutive re-use cycles proved effective, both emphasize their viability as bio-sorbents.

Acknowledgments

The authors gratefully acknowledge the National Council for Scientific and Technological Development (CNPq), the Coordination for the Improvement of Higher Level (CAPES), the Minas Gerais State Research Foundation (FAPEMIG) and Financier of Studies and Projects (FINEP).

REFERENCES

[1] Klen, M. R. F., Cervelin, P. C., Veit, M. T., Gonçalves, G. C., Bergamasco, R., Silva, F. V. (2012) Adsorption kinetics of blue 5G dye from aqueous solution on dead floating aquatic macrophyte: Effect of pH, temperature, and

pretreatment. Water, Air, Soil Pollut, 223, 4369-4381. [http://link.springer.com/article/10.1007%2Fs11270-012-1201-x#page-1]

[2] Wu, Q., Feng, C., Wang, C., Wang, Z. (2013) A facile one-pot solvothermal method to produce superparamagnetic graphene-Fe3O4 nanocomposite and its application in the removal of dye from aqueous solution. Colloids Surf. B, 101, 210-214. [http://www.ncbi.nlm.nih.gov/pubmed/23010021]

[3] Bestani, B., Benderdouche, N., Benstaali, B., Belhakem, M., Addou, A. (2008) Methylene blue and iodine adsorption onto an activated desert plant. Bioresour.Technol. 99, 8441-8444. [http://www.sciencedirect.com/science/article/pii/S0960852408001983]

[4] Dallago, R. M., Smaniotto, A., Oliveira, L. C. (2005) Resíduos Sólidos de Curtumes como adsorventes para a Remoção de Corantes em Meio Aquoso. Quim. Nova, 28, 433-437. [http://abqct.com.br/artigost/artigoesp32.pdf]

[5] Abdallah, R., Taha, S. (2012) Biosorption of methylene blue from aqueous solution by nonviable Aspergillus fumigates. Chem. Eng. J. 195-196, 69-76. [http://www.sciencedirect.com/science/article/pii/S1385894712005281]

[6] Fan, L., Zhou, Y., Yang, W., Chen, G., Yang, F. (2008) Electrochemical degradation of aqueous solution of Amaranth azo dye on ACF under potentiostatic model. Dyes Pigm. 76, 440–446. [http://www.sciencedirect.com/science/article/pii/S0143720806003895]

[7] Sudarjanto, G., Keller-Lehmann, B., Keller, J. (2006) Optimization of integrated chemical–biological degradation of a reactive azo dye using response surface methodology. J. Hazard. Mater. 138, 160–168. [http://www.ncbi.nlm.nih.gov/pubmed/16814466]

[8] Ofomaia, A. E., Ukpebor, E. E., Uzoekwe, S. A. (2011) Biosorption of methyl violet onto palm Kernel fiber: Diffusion studies and multistage process design to minimize biosobent mass and contact time, Biomass Bioenergy. 35, 4112-4123. [http://www.researchgate.net/publication/251629067_Biosorption_of_Methyl_violet_onto_palm_kernel_fiber_Diffusion_studies_and_multistage_process_design_to_minimize_biosorbent_mass_and_contact_time]

[9] Lodha B., Chaudhari, S. (2007) Optimization of Fenton-biological treatment scheme for the treatment of aqueous dye solutions. J. Hazard. Mater. 148, 459-466. [http://www.ncbi.nlm.nih.gov/pubmed/17403567]

[10] Dogan, M., Ozdemir, Y., Alkan, M. (2007) Adsorption kinetics and mechanism of cationic methyl violet and methylene blue dyes onto sepiolite. Dyes Pigm.75, 701-713. [http://www.sciencedirect.com/science/article/pii/S014372080600307X]

[11] Rafatullaha, M., Sulaimana, O., Hashima, R., Ahmadb, A. (2010) Adsorption of methylene blue on low cost adsorbents: A review. J. Hazard. Mater. 177, 70–80. [http://www.sciencedirect.com/science/article/pii/S0304389409020354]

[12] Singh, K. P., Mohan, D., Sinha, S., Tondon, G. S., Gosh, D. (2003) Color removal from wastewater using low-cost activated carbon derived from agricultural waste material. Ind. Eng. Chem. Res. 42, 1965-1976. [http://pubs.acs.org/doi/abs/10.1021/ie020800d]

[13] Carvalho, W. S., Martins, D. F., Gomes, F. R., Leite, I. R., da Silva, L. G., Rugguero, R., Richter, E. M. (2011) Phosphate adsorption on chemically modified sugarcane bagasse fibres. Biomass Bioenergy. 35, 3913-3919. http://www.researchgate.net/publication/232407321_Phosphate_adsorption_on_chemically_modified_sugarcane_bagasse_fibres]

[14] Phan, N. H., Rio, S., Faur, C., Le Coq, L., Le Cloirec, P., Nguyen, T. H. (2006) Production of fibrous activated carbons from natural cellulose (jute, coconut) fibers for water treatment applications. Carbon. 44, 2569-2577. [http://www.sciencedirect.com/science/article/pii/S0008622306003150]

[15] Franca, A. S., Oliveira, L. S., Ferreira, M. E. (2009) Kinetics and equilibrium studies of methylene blue adsorption by spent coffee grounds. Desalination. 249, 267-272. [http://www.sciencedirect.com/science/article/pii/S0011916409008376]

[16] Vieira, S. S., Magriotis, Z. M., Santos, N. A. V., Cardoso, M. G., Saczk, A. A. (2012) Macauba palm (Acrocomia aculeata) cake from biodiesel processing: An efficient and low cost substrate for the adsorption of dyes. Chem. Eng. J. 183, 152-161. [http://www.sciencedirect.com/science/article/pii/S138589471101597X]

[17] Chowdhury, S., Mishra, R., Saha, P., Kushwaha, P. (2011) Adsorption thermodynamics, kinetics and isosteric heat of adsorption of malachite green onto chemically modified rice husk. Desalination. 265, 158-168. [http://www.sciencedirect.com/science/article/pii/S001191641000545X]

[18] Sun, X. F., Xu, F., Sun, R. C., Fowler, P., Baird, M. S. (2005) Characteristics of degraded cellulose obtained from steam-exploded wheat straw. Carbohydrate Research. 340, 97-106. [http://www.sciencedirect.com/science/article/pii/S0008621504004616]

[19] Rubio, J., Schneider I. A. H., Ribeiro, Costa, T., C. A., Kallfez, C. A. (2004) Plantas Aquáticas: Sorventes Naturais. Rev. Cienc. Hoje, 35, 68–71. [http://www.petronews.com.br/download.php?recid=52]

[20] Royer, B., Cardoso, N. F., Lima, E. C., Vaghetti, J. C. P., Simon, N. M., Calvete, T., Veses, R. C. (2009) Applications of Brazilian-pine fruit shell in natural and carbonized forms as adsorbents to removal methylene blue from aqueous solutions - kinetic and equilibrium study. J. Hazard. Mater. 164, 1213-1222. [http://www.ncbi.nlm.nih.gov/pubmed/18930589]

[21] Kumar, K. V., Porkodi, K. (2006) Relation between some two- and three-parameter isotherm models for the sorption of methylene blue onto lemon peel. J. Hazard. Mater. 138, 633–635. [http://www.sciencedirect.com/science/article/pii/S0304389406007205]

[22] Kumar, P. S., Ramalingam, V., Sathishkumar, V. (2011) Removal of methylene blue dye from aqueous solution by activated carbon prepared from cashew nut shell as a new low-cost adsorbent, Korean. Chem. Eng. J. 28, 149–155. [http://link.springer.com/article/10.1007%2Fs11814-010-0342-0#page-1]

[23] Yang, J., Qiu, K. (2010) Preparation of activated carbons from walnut shells via vacuum chemical activation and their application for methylene blue removal. Chem. Eng. J. 165, 209–217. [http://www.sciencedirect.com/science/article/pii/S1385894710008491]

[24] Al-Anber, Z. A., Al-Anber, M. A., Matouq, M., Al-Ayed, O., Omari, N. M. (2011) Defatted Jojoba for the removal of methylene blue from aqueous solution: Thermodynamic and kinetic studies. Desalination. 276, 169–174. [http://www.sciencedirect.com/science/article/pii/S001191641100261X]

[25] Belala, Z., Jeguirim, M., Belhachemi, M., Addoun, F., Trouvé, G. (2011) Biosorption of basic dye from aqueous solutions by Date Stones and Palm-Trees Waste: Kinetic, equilibrium and thermodynamic studies. Desalination. 271, 80–87. [http://www.sciencedirect.com/science/article/pii/S0011916410009161]

[26] Kumar, K. V., Kumaran, A. (2005) Removal of methylene blue by mango seed kernel powder. Bioch. Eng. J. 27, 83–93. [http://www.sciencedirect.com/science/article/pii/S1369703X05002342]

[27] Lagergren, S. (1898) About the theory of so-called adsorption of soluble substance, K. Sven. Vetenskapsakad. Handl. 24, 1-39. [About the theory of so-called adsorption of soluble substance]

[28] Ho, Y. S., Mckay, G. (1999) Pseudo-second order model for sorption process. Process Biochem., 34, 451-465. [http://www.sciencedirect.com/science/article/pii/S0032959298001125]

[29] Weber, W. J., Morris, J. C. (1963) Kinetics of adsorption on carbon from solution, J. Sanit. Eng. 89, 31-59. [http://cedb.asce.org/cgi/WWWdisplay.cgi?13042]

[30] Juang, R. S., Chen, M. L. (1997) Applicationof the Elovich equation to the kinetics of metal sorption with solvent-impregnated resins. Chem. Eng. J. 36, 813-820. [http://pubs.acs.org/doi/abs/10.1021/ie960351f]

[31] Lopes, E. C. N., dos Anjos, F. S. C., Vieira, E. F. S., Cestari, A. R. (2003) An alternative Avrami equation to evaluate kinetic parameters of the interaction of Hg(II) with thin chitosan membranes. J.Colloid Interface Sci. 263, 542-547. [http://www.sciencedirect.com/science/article/pii/S0021979703003266]

[32] Langmuir, I. (1918) The adsoption of gases on plane surfaces of glass, mica and platinum, J. Am. Chem.So. 40, 1361-1403. [http://pubs.acs.org/doi/abs/10.1021/ja02242a004]

[33] Freundlich, H. M. F. (1906) Over the adsorption in solution, J. Phys. Chem. 57, 385-471.

[34] Sips, R., (1948) Combined from of Langmuir and Freundlich equations. J. Chem. Phys. 16, 490-495.

[35] Dubinin, M. M. (1960) The Potential Theory of Adsoption of Gases and Vapors for Adsorbents with Energetically non uniforms Surfaces. Chem. Rev. 60, 235-241. [http://www.researchgate.net/publication/231246767_The_Potential_Theory_of_Adsorption_of_Gases_and_Vapors_for_Adsorbents_with_Energetically_Nonuniform_Surfaces]